


GCMs simulation-based assessment for the response of the Mediterranean Gaza coastal aquifer to climate-induced changes

Hassan Al-Najjar ^{a,*}, Gokmen Ceribasib^b, Emrah Dogan^c, Ahmet Iyad Ceyhunlu^b, Mazen Abualtayef^d and Khalid Qahman^e

^a Department of Civil Engineering, Institute of Natural Sciences, Sakarya University, 54187 Sakarya, Turkey

^b Department of Civil Engineering, Technology Faculty, Sakarya University of Applied Sciences, 54187 Sakarya, Turkey

^c Department of Civil Engineering, Faculty of Engineering, Sakarya University, 54187 Sakarya, Turkey

^d Department of Civil Engineering, Faculty of Engineering, Islamic University of Gaza, Gaza, Palestine

^e Environment Quality Authority, Gaza, Palestine

*Corresponding author. E-mail: hassan.al-najjar@ogr.sakarya.edu.tr

 HA, 0000-0003-2192-4301

ABSTRACT

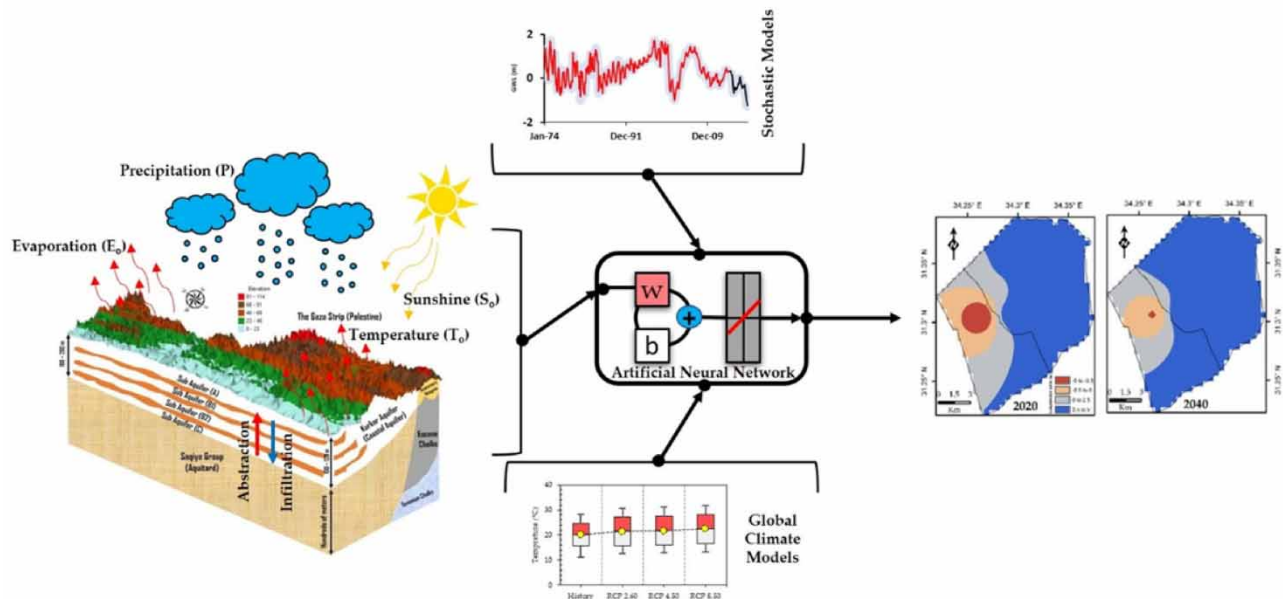
In the Eastern Mediterranean countries, groundwater contained in coastal aquifers is the predominant water source for supplying water. The Mediterranean Gaza coastal aquifer in Palestine is showing alarming signs of depletion due to climate change and human-caused influences that substantially impact the hydraulic performance of the Gaza coastal aquifer. The climate statistical modeling and the downscaling of the ensemble global climate model under the representative concentration pathway (RCP) scenarios of RCP 2.60, 4.50, and 8.50 refer to a future decreasing trend in the precipitation and an increasing trend in the temperature. The stochastic model refers to an average decrease of -5.2% in the rainfall every 20 years that coincides with the RCP scenarios that show a decrease in precipitation between 0 and -5% . The rate of temperature increase over the next 20 years is defined at $+1\text{ }^{\circ}\text{C}$, which closely matches the RCP results. As a result of human fast-paced activities, groundwater consumption is expected to rise by nearly 55% by the end of 2040, to around 193 million cubic meters, with a substantial withdrawal trend in southern provinces of the Gaza Strip. Consequently, the aquifer model predicts that subsurface water levels might fall at a rate of -2.50% per year, reaching a level of around -27.77 m below the mean sea level (MSL) by 2040. Alternative water supplies, such as desalinated seawater and treated wastewater, with annual maximum volumes of 110 and 16.5 million cubic meters, respectively, are expected to perfectly recharge groundwater resources of the Gaza coastal aquifer at an annual rate of about $+3.65\%$ to meet a groundwater table level of around -5 m below the MSL by 2040.

Key words: aquifer, climate, GCMs, Palestine, simulation, statistic

HIGHLIGHTS

- The stochastic and global circulation models (GCMs) show a decadal climate trend of a $0.5\text{ }^{\circ}\text{C}$ increase in temperature and a -2.5% decline in total monthly precipitation in the eastern Mediterranean coastal areas.
- The coastal aquifers are the main water source for supplying water in Mediterranean regions.
- Seawater desalination and wastewater reclamation are long-term strategies for alleviating the consequences of water stress.

GRAPHICAL ABSTRACT



1. INTRODUCTION

Arid and semi-arid areas, home to around 2000 million people or roughly 30% of the world's population who consume about 1,500,000 million cubic meters of fully tapped groundwater, are experiencing catastrophic water shortages and severe climate aridity (Burek *et al.* 2013; Dogrul *et al.* 2016; Anderson 2017; Hussain *et al.* 2019; Al-Najjar *et al.* 2020). The coastal Mediterranean aquifers are unique and the only water resource used for water supply services in the Middle East and North Africa where the threats of climate disturbances and overuse practices led to crucial deficiencies in terms of water and food security where the groundwater surveillance systems refer to a dangerous drop in the groundwater table to levels below the mean sea level, which, in turn, result in excessive seawater invasion and prolonged salinization (Ye *et al.* 2015; Dogrul *et al.* 2016; Zekri *et al.* 2017; Otkin *et al.* 2018; Schiermeier 2018; Gopalakrishnan *et al.* 2019; Hussain *et al.* 2019; Al-Najjar *et al.* 2021a, 2021b). As a result, new nontraditional water resources provided through seawater desalination and wastewater treatment industries are considerably identified as promising practical options to alleviate the continuous deterioration in the groundwater balance and close up the gap in the water budget (Al-Najjar *et al.* 2021a). Globally, seawater desalination technologies provide 32,500 million cubic meters of freshwater per year, or about 0.7% of global water needs. Wastewater treatment and reuse are widely used for agricultural irrigation and groundwater recharge in Australia, China, the United States (California and Florida), and the Arabian Gulf, with an annual treatment capacity of 280, 14,000, 1750, and 2800 million cubic meters, respectively. Specifically, setting a modeling basis for analyzing climate and human-induced effects on coastal aquifer underground water resources is critical for an effective groundwater management system that aims to adopt efficient policies and mitigation measures to remediate any hazardous effects on groundwater sustainable practices (Ye *et al.* 2015; Karimi *et al.* 2019). Climate models, which are primarily represented by global circulation models (GCMs), are spatially downscaled to a regional scale based on scenarios of greenhouse emissions by using local data acquired from ground meteorological stations to predict the future tendency of the climate. The fifth phase project of the coupled model intercomparison project (CIMP5) was developed based on four climate scenarios demonstrated by representative concentration pathways (RCPs) for the greenhouse gas concentrations trajectory adopted by the intergovernmental panel on climate change (IPCC), which are RCP 2.6, 4.5, 6.0, and 8.5 (IPCC 2019). Overcoming the shortcomings and complexity of groundwater numerical models, data-driven models are merit simulators for incorporating the various aspects that influence a groundwater system dynamic response (Butler *et al.* 2013; Yeh & Chang 2013; Singh 2014; Djurovic *et al.* 2015; Gladden & Park 2016; Thangarajan & Singh 2016). A stochastic serial dependent analysis is used to simulate the climate and groundwater time series to anticipate the

future trend based on the inherent tendency of historical observations to design a representative statistical data model (Adamowski *et al.* 2012; Sahoo & Jha 2013; Kumbuyo *et al.* 2014; Mirzavand & Ghazavi 2015; Mogaji *et al.* 2015; Patle *et al.* 2015; Yan & Ma 2016; Zhou *et al.* 2017; Al-Najjar *et al.* 2020, 2021b). The intelligent artificial data-driven algorithmic approaches, which can describe the complex relationship between multi-input and output parameters, have been used to accurately detect the nonlinear behavior between climatic parameters and the response of the groundwater level (Emamgholizadeh *et al.* 2014; Afan *et al.* 2015; Chang *et al.* 2016; Sun *et al.* 2016; Ebrahimi & Rajaei 2017). The stochastic autoregressive integrated moving average (ARIMA) is a famous statistical model established based on the autoregression concept, which allows for the extraction of information from time-series data through autocorrelation analysis functions (Box & Jenkins 1970; Koopmans 1974; Kashyap & Rao 1976; Box *et al.* 2008; Chatfield 2008; Kumbuyo *et al.* 2014; Al-Najjar *et al.* 2020, 2021b). Numerous studies in the field of water and climate modeling have addressed the stochastic ARIMA models (Bazrafshan *et al.* 2015; Mirzavand & Ghazavi 2015; Djerbouai & Souag-Gamane 2016; Khorasani *et al.* 2016; Myronidis *et al.* 2018; Takafuji *et al.* 2018; Sakizadeh *et al.* 2019; Al-Najjar *et al.* 2020, 2021a, 2021b). Artificial neural networks (ANNs) are data-driven networks with neurons that receive, process, and transmit information from the input layer to the output layer. The logistic sigmoid function network of multi-layer feed-forward perceptron (MLP) with a single hidden layer is normally advised as a model for predicting water and climate interactions by numerous studies (Maier *et al.* 2010; Mohanty *et al.* 2010; Adamowski & Chan 2011; Chen *et al.* 2011; Jalalkamali *et al.* 2011; Nourani *et al.* 2011; Trichakis *et al.* 2011; Yoon *et al.* 2011; Rakhshandehroo *et al.* 2012; Taormina *et al.* 2012; Moosavi *et al.* 2013; Sahoo & Jha 2013; Shirmohammadi *et al.* 2013; Emamgholizadeh *et al.* 2014; He *et al.* 2014; Tapoglou *et al.* 2014; Ying *et al.* 2014; Juan *et al.* 2015; Khaki *et al.* 2015; Khalil *et al.* 2015; Mohanty *et al.* 2015; Nourani *et al.* 2015; Yang *et al.* 2015; Gong *et al.* 2016; Nourani & Mousavi 2016; Sun *et al.* 2016; Yoon *et al.* 2016; Barzegar *et al.* 2017; Ebrahimi & Rajaei 2017; Wen *et al.* 2017; Ghose *et al.* 2018; Kouziokas *et al.* 2018; Yu *et al.* 2018; Guzman *et al.* 2019; Lee *et al.* 2019; Tang *et al.* 2019; Al-Najjar *et al.* 2021a, 2021b). In the Gaza Strip of Palestine, due to excessive water pumping and limited precipitation as a result of rising temperatures, the Gaza coastal aquifer, which is the only available water resource for water supply in the Gaza Strip, is anticipated to be severely strained throughout the mid-future. Due to the ambiguity of climate variations, this study used a simulation-based approach to assess potential changes in climate conditions and future impacts of climate and anthropogenic practices on Gaza coastal aquifer groundwater table fluctuations, as well as the impact of alternative water resources, such as seawater desalination and wastewater treatment, on groundwater resource recovery.

2. CLIMATE AND GROUNDWATER IN THE STUDY AREA

The Gaza Strip, as shown in Figure 1, is a 365 km² coastal strip of land located on the Mediterranean Sea's southeast coast, stretching 42 km and varying in width from 6 to 12 km. With a population of more than two million people, the Gaza Strip is considered one of the world's most densely populated areas (Palestinian Central Bureau of Statistics (PCBS) 2020). The Gaza Strip's water supply system is semi-collapsed with the only source of water being severely contaminated and deteriorating as a result of unsustainable pumping of roughly 200 million cubic meters per year (PWA 2011, 2012, 2014, 2015; UN 2012). Drought has become more common in the Gaza Strip as a result of climate change's effects, which have harmed the coastal aquifer's vulnerability and the viability of agricultural activities where the drought investigation studies refer to an increase in the incidence of drought occurrence from about 20% in the 1970s to more than 80% in the last 10 years (Al-Najjar *et al.* 2020). The Palestinian Water Authority (PWA) has established water management strategies and mitigation measures, as shown in Figure 2, to deal with the Gaza Strip's water shortage in response to the effects of climate change and anthropogenic concerns. The proposed intervention management plans include the construction of three seawater desalination plants to provide 13 million cubic meters of water per year, as well as the construction of a large-scale seawater desalination plant to provide 110–120 million cubic meters per year, to reduce water abstraction from the coastal aquifer by about 35–60% over the next 20 years (PWA 2011, 2014; UfM 2011; Abuatayef *et al.* 2016).

In parallel to this, the PWA approved a long-term strategic plan to build three large-scale wastewater treatment plants to support the agricultural sector with about 75 million cubic meters of treated water for irrigation and to cope with the drought impact, as well as to reduce groundwater abstraction from the coastal aquifer by about half, from 180 to about 70 million cubic meters per year by 2032 (PWA 2011, 2013, 2014; Abuatayef *et al.* 2020).

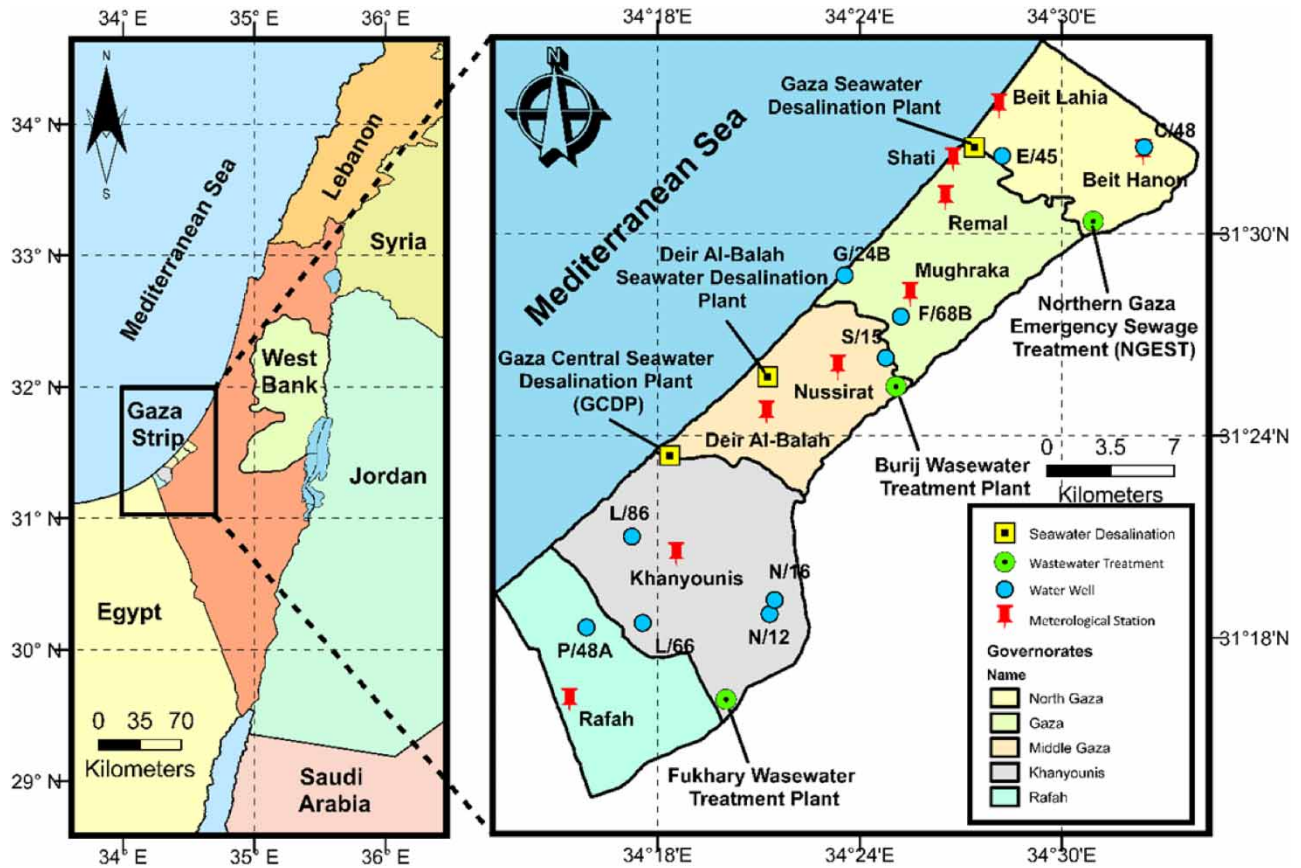


Figure 1 | Location of climate and water monitoring and practices in the Gaza Strip.

3. MATHEMATICAL ALGORITHMS

3.1. Mathematical models

The mathematical expression of the Box–Jenkins ARIMA model is described in Equation (1) (Box & Jenkins 1976; Kottegoda 1990; Tong 1990; Shahin *et al.* 1993; Polyak 1996; Sharma *et al.* 2019; Al-Najjar *et al.* 2020):

$$\left[1 - \sum_{i=1}^p \phi_i B^i \right] \left[1 - \sum_{i=1}^P \phi_{is} B^{i \times S} \right] (1 - B)^d (1 - B^S)^D x_t = \left[1 + \sum_{i=1}^q \theta_i B^i \right] \left[1 + \sum_{i=1}^Q \theta_{is} B^{i \times S} \right] \varepsilon_t \quad (1)$$

where ϕ_i is the i th autoregressive (AR) parameter; ϕ_{is} is the i th seasonal AR parameter; θ_i is the i th moving average (MA) parameter; θ_{is} is the i th seasonal MA parameter; B is the backshift operator; d is the differencing; D is the seasonal differencing; S is the seasonality period; and ε_t is a noise random component.

The artificial network of MLP with a single hidden layer is mathematically demonstrated by Equation (2) based on the logistic sigmoid activation function (Bishop 1995; Haykin 2009; Sahoo & Jha 2013):

$$\varphi \left(\sum_{j=1}^l w_{jk} z_j + b_j \right) = \frac{1}{1 + e^{-\left(\sum_{j=1}^l w_{jk} z_j + b_j \right)}} \quad (2)$$

where w_{jk} is the connection weight between the j th node of the hidden layer and the output node k ; z_j is the output of the j th hidden neuron resulting from the input data; and b_j is the connection weight for bias term.

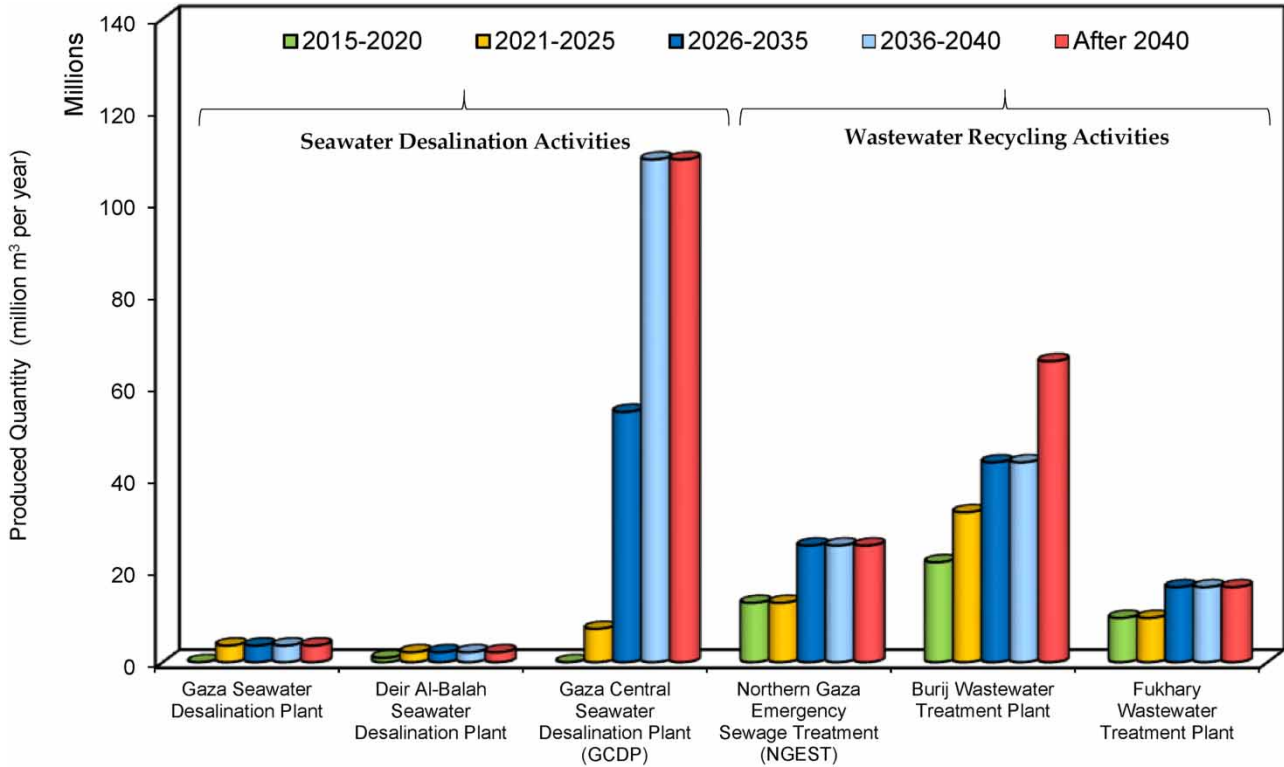


Figure 2 | Seawater desalination and wastewater recycling in the Gaza Strip.

3.2. Performance tests

The evaluation of the models’ performance was addressed by the correlation coefficient (r) (Equation (3)), the root mean square error ($RMSE$) (Equation (4)), Nash–Sutcliffe model efficiency coefficient (NSE) (Equation (5)), refined index of agreement (d'_1) (Equation (6)), and Thiel’s index of inequality (TU) (Equation (7)), as shown in the following:

$$\text{Correlation coefficient } (r) = \frac{\sum_i^N (actual_i - \overline{actual})(predicted_i - \overline{predicted})}{\sqrt{\sum_i^N (actual_i - \overline{actual})^2 \sum_i^N (predicted_i - \overline{predicted})^2}} \tag{3}$$

$$RMSE = \sqrt{\frac{\sum_{i=1}^N (predicted_i - actual_i)^2}{N}} \tag{4}$$

$$NSE = 1 - \frac{\sum_{i=1}^N (actual_i - predicted_i)^2}{\sum_{i=1}^N (actual_i - \overline{actual_i})^2} \tag{5}$$

$$d'_1 = 1 - \frac{\sum_{i=1}^N |predicted_i - actual_i|}{2 \sum_{i=1}^N |actual_i - \overline{actual}|} \tag{6}$$

$$TU = \left[\frac{\sum_{i=1}^N (actual_i - predicted_i)}{\sum_{i=1}^N (actual_i)^2} \right]^{1/2} \tag{7}$$

where $actual_i$ is the actual i th observed data and $predicted_i$ is the predicted i th simulated data.

4. MATERIAL AND METHODS

Historical total monthly based raw data for the climate parameter of precipitation (P_o) were obtained from nine meteorological stations located inside the geographical extent of the Gaza Strip from January 1974 to December 2020. Furthermore, the available monthly time-series data for the climate parameters of minimum temperature (T_{min}), average temperature (T_{avg}), maximum temperature (T_{max}), sunshine (S_o), evaporation (E_o), and humidity (H_o) are regularly measured only at the Remal meteorological station and were gathered from January 1974 to December 2006. For groundwater condition analysis, the time series for the municipal monthly groundwater consumption (C_o) from January 1997 to December 2011 were retrieved from the metered records of the monthly groundwater pumping. In addition, available measurements for the monthly fluctuating level of the mean sea level (MSL) groundwater table response (R) were obtained from 10 piezometric groundwater wells for the period from January 1974 to December 2018. Each class of time-series data was statistically processed and temporally standardized over the period from January 1974 to December 2040 using ARIMA stochastic models. The ensemble climate model of CIMP5 was regionally downscaled for the parameters of monthly rainfall and average temperature under three greenhouse gas emission scenarios of RCPs of 2.60, 4.50, and 8.50. The artificial one hidden layer feed-forward backpropagation MLP network of 20 neurons was structured to combine the impact of the climate and human factors on the groundwater level of the Mediterranean Gaza coastal aquifer. The new quantities of the alternative water resources deriving from seawater desalination and wastewater treatment were simulated by reducing the groundwater consumption by the amount of the supplementary water supply.

5. ANALYSIS OF RESULTS

5.1. Analysis of climate data

The available historical records for the total monthly precipitation (P_o) are presented in the heat maps, as shown in Figure 3. According to the analysis, the Gaza Strip is a low-rainfall region, with the maximum total monthly rainfall of less than 330 mm throughout the rainy season, which spans from November to March.

The future projection of the precipitation in the Gaza Strip up to the year 2098 is presented in the boxplot of Figure 4. The regional trend indicates a decreasing manner in the total rainfall from the north to the south of the Gaza Strip as well as the future projection refers to a decreasing temporal trend over 2006–2036, 2037–2067, and 2068–2098.

The geographical distribution for the variation in the total rainfall, as shown in Figure 5, reveals a decreasing trend in the total rainfall over the near and far future. Hence, the variation in the rainfall throughout 2006–2036 compared to the base period of 1975–2005 is within 0 to –5% for the RCP 2.60, while the variation is assigned to –5 to –15% and –15 to –25% for the RCP of 4.50 and 8.50, respectively.

The available historical records for the minimum temperature (T_{min}), average temperature (T_{avg}), and maximum temperature (T_{max}) were determined in the heat maps, as shown in Figure 6. The temperature in the area of the Gaza Strip fluctuates between about 7 °C in cold seasons and 35 °C in hot seasons.

The future downscaling of ensemble GCM of CIMP5 for the average temperature, as shown in Figure 7, indicates an increasing trend by about +1 °C within 2006–2036 above the average temperature of 20 °C recorded throughout 1975–2005. However, throughout 2037–2067, the incremental increase in temperature is expected to be +1 °C above the average temperature recorded during 1975–2005. However, by 2068–2098, the temperature increase is probable to reach +4 °C above the average temperature recorded during 1975–2005.

The stochastic ARIMA models for the climate parameters are depicted in Figure 8 in terms of calibration and validation and Table 1 for models' terms of seasonal and nonseasonal parameters. The ARIMA models show accurate simulation for the climate parameters with accuracy ranges between 74 and 99%.

To provide cross-validation for the results of ARIMA models, a comparison was performed throughout 2006–2036 for the parameters of precipitation and average temperature, as shown in Figure 9. For the parameter of precipitation, the deviation of the ARIMA outputs to the outputs of the RCP scenarios is about +7%. However, in the parameter of temperature, the deviation is assigned to +8.5%.

5.2. Analysis of groundwater consumption

The extraction of groundwater from drilling wells throughout the Gaza Strip has a substantial influence on the water budget of the Gaza coastal aquifer and is the main cause of groundwater storage instability. This research recommends using the

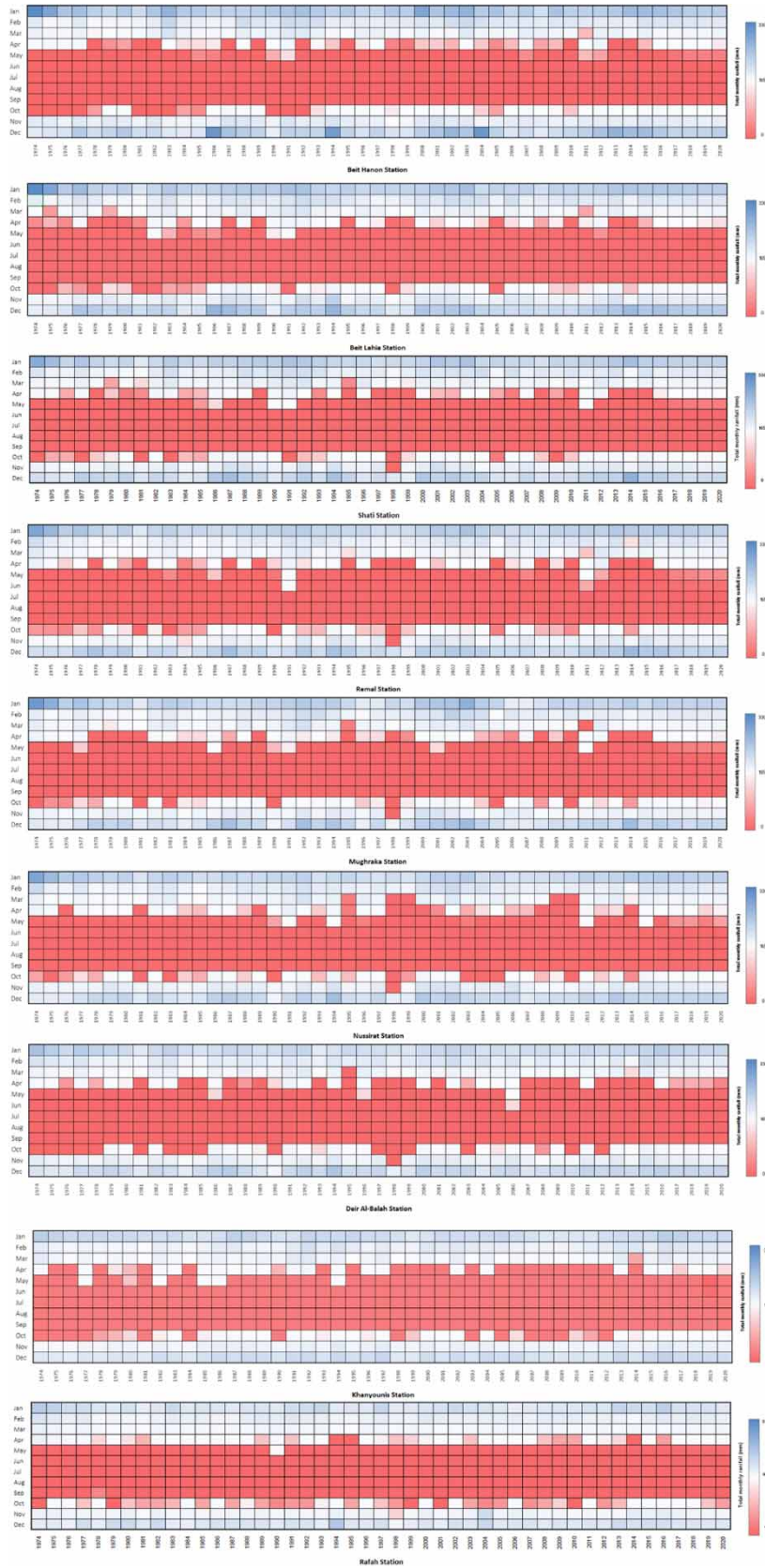


Figure 3 | Time-series of total monthly rainfall.

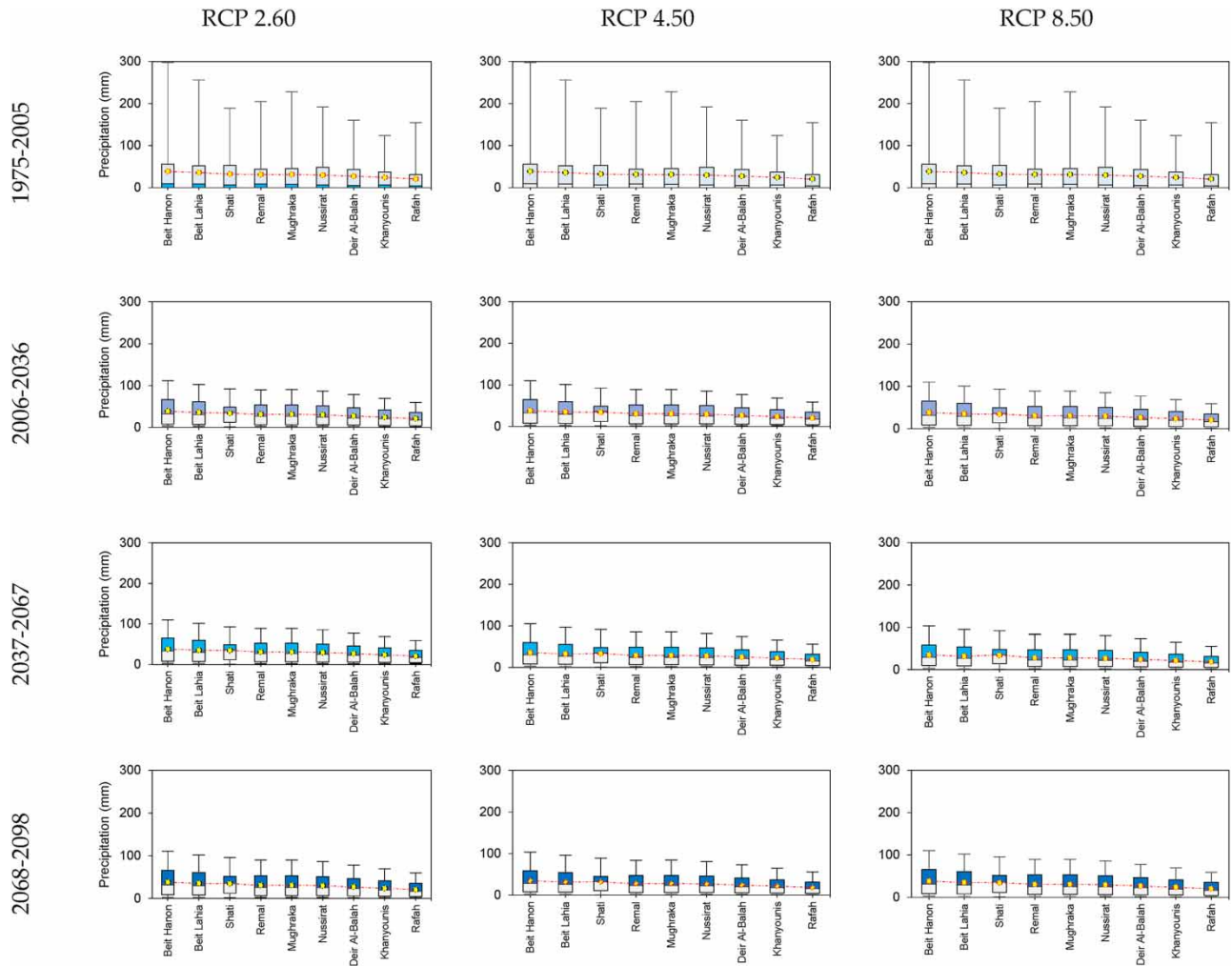


Figure 4 | Boxplot statistical analysis for the total monthly rainfall under the RCP scenarios over 1975–2098.

stochastic ARIMA model of $(2,1,5) (2,1,1)_{12}$ to forecast and back-cast the time series of groundwater extraction from the Gaza coastal aquifer at each Gaza Strip governorate to lengthen the time series and give a deeper understanding of groundwater hydraulic behavior and actions. As shown in Figure 10, the stochastic model predicts that groundwater utilization began in the Gaza Strip's northern governorates in 1986. The extraction of groundwater began in the Gaza governorate in the mid-1970s, while the southern governorates began using it around the end of the 1980s and the beginning of the 1990s. Recently, groundwater extraction has been observed in a rapid and widespread way, particularly in the southern governorates of the Gaza Strip.

The stochastic model offers an ideal simulation for the time series of groundwater extraction quantities, with a correlation coefficient (r) of above 90%. Groundwater extraction practice reveals an annual increasing tendency that varies by location by roughly 12–59%, with an overall average of 24%. The agricultural methods in the Gaza Strip's northern governorates encourage rapid groundwater extraction, which puts pressure on the Gaza coastal aquifer.

5.3. Analysis of groundwater level

The dominant feature that determines the interplay between the various physical factors in nature is a nonlinear function. Due to the obvious complexity of the association between meteorological and hydrological indicators, numerous scientific approaches have been proposed and coupled to interpret the intrinsic relationship between these factors. Therefore, the

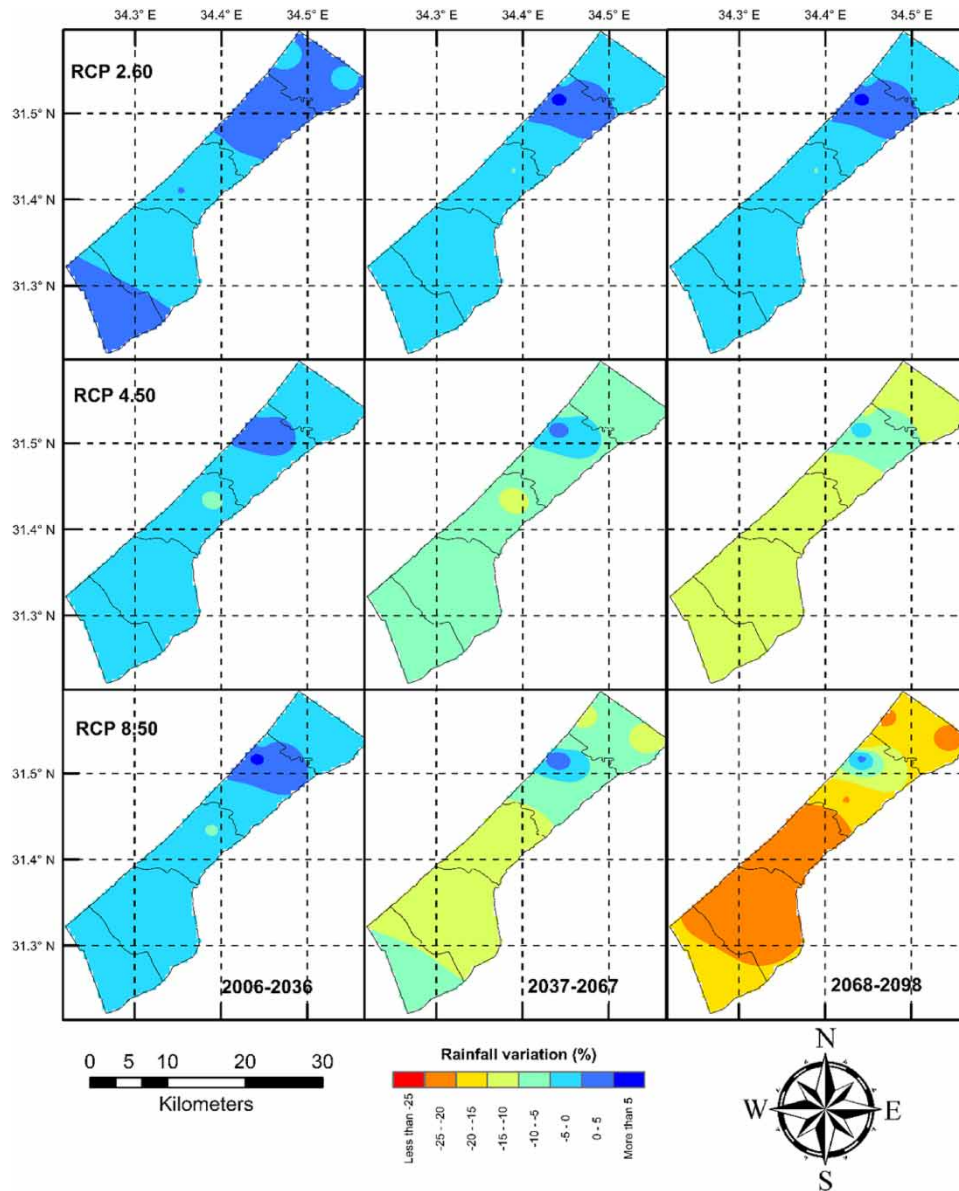


Figure 5 | Geographical distribution of the total monthly rainfall under the RCP scenarios over 1975–2098.

artificial MLP approach, as shown in [Figure 11](#), was exploited to model the response of the Gaza coastal aquifer to the climate and human-induced changes.

The network was developed by training the network on 540 combinations of the data for each time series of the 10 groundwater wells. In terms of performance testing, it shows a valid presentation of the observed groundwater level. In an overall manner, as shown in [Figures 12](#) and [13](#), the stochastic models describe the relationship between the observed and the simulated data by a correlation coefficient (r) of 95–99%, $RMSE$ of 0.1–0.22, and NSE of 0.93–0.99

The parameters of performance testing for the calibration and validation are illustrated in [Table 2](#).

The Gaza Strip's southern region seems to be the most densely populated region of the area. The local wells produce groundwater at a volume of far more than 100 m³ per hour, which negatively affects the availability of the Gaza coastal

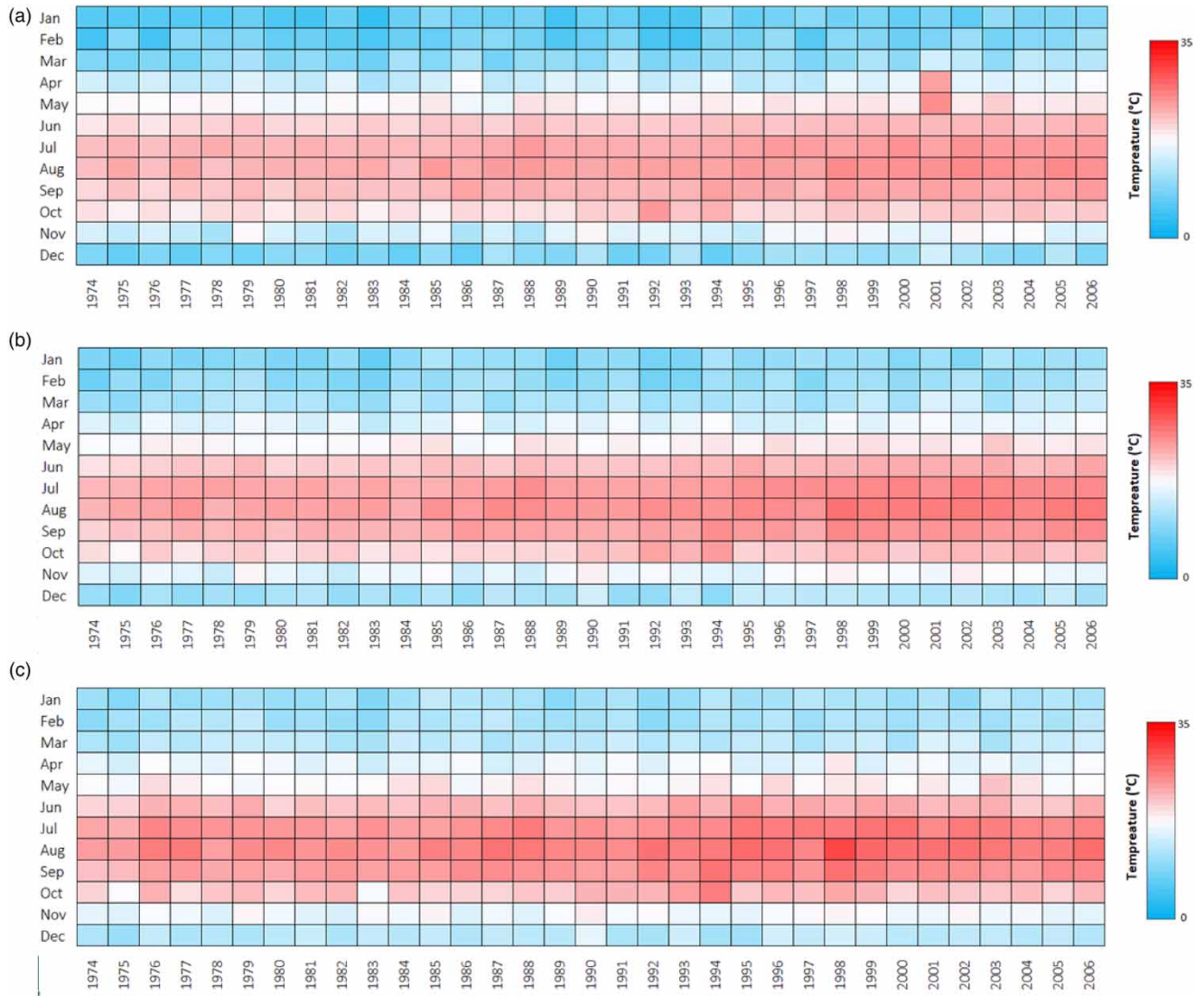


Figure 6 | Time series over 1974–2006 for (a) minimum temperature (T_{min}), (b) average temperature (T_{avg}), and (c) maximum temperature (T_{max}).

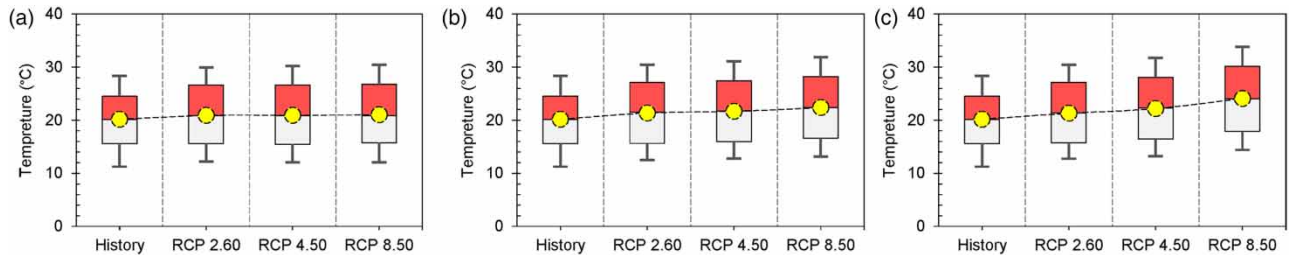


Figure 7 | Boxplot statistical analysis for the average temperature under the RCP scenarios for (a) 2006–2036, (b) 2037–2067, and (c) 2068–2098.

aquifer in this area. The groundwater depletion cone started to form in the Gaza Strip in 1992, and it has been spreading northward ever since. The cone’s diameter was less than 1 km in 1992, and it is anticipated to grow to 4–5 km by 2040. As a result, seawater intrusion is the most common phenomenon that has an impact on groundwater quality by lowering

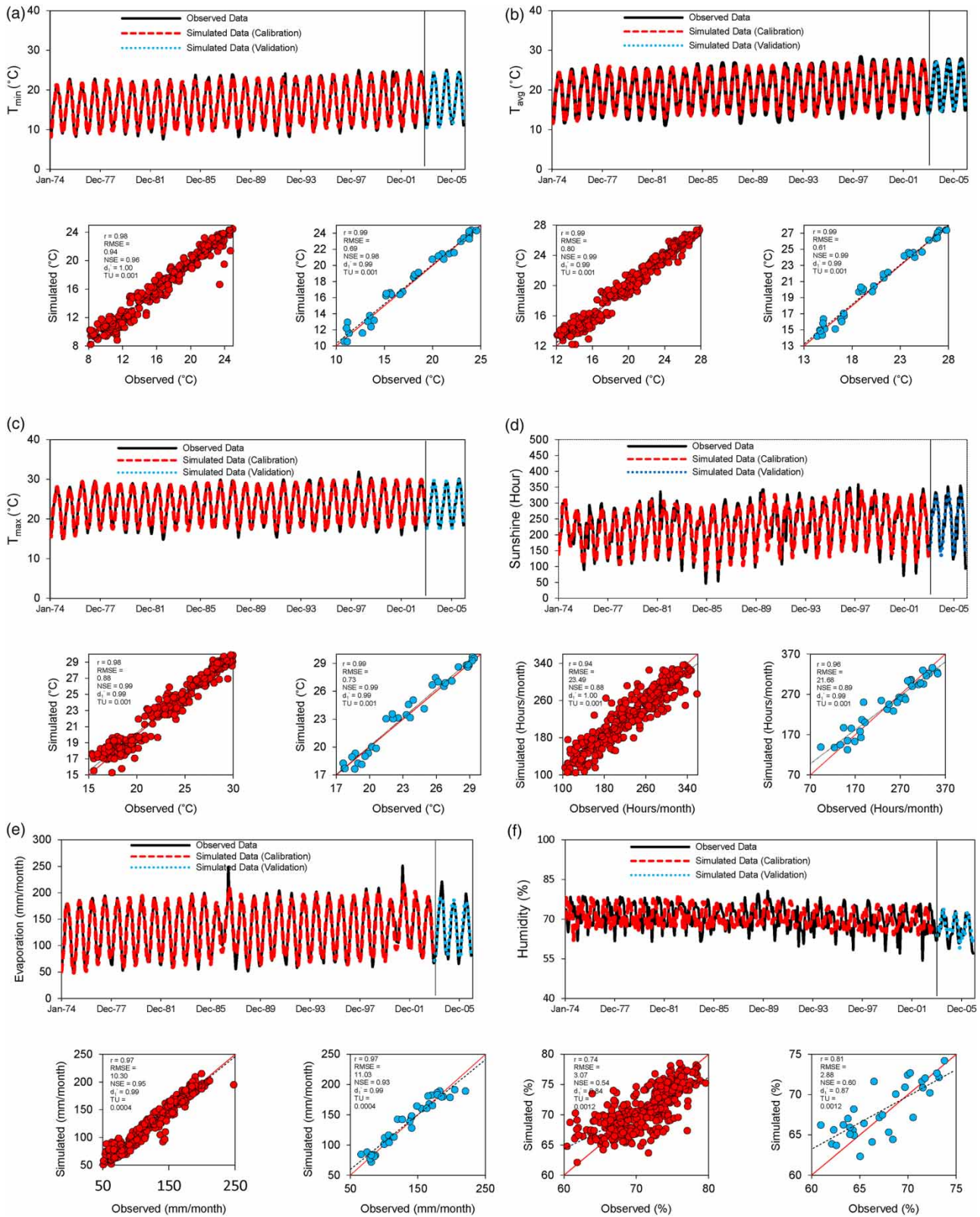


Figure 8 | Time series over 1974–2006 for (a) minimum temperature, (b) average temperature, and (c) maximum temperature.

Table 1 | The model AR and MA parameters for the climate parameters

Factor	Model	Class	Φ_1	Φ_2	Φ_3	Φ_4	Φ_5	θ_1	θ_2	θ_3	θ_4	θ_5
T_{min}	(3,1,2) (2,1,1) ₁₂	Seasonal	0.8972	-0.273	0.0476	-	-	-1.5116	0.5117	-	-	-
		Nonseasonal	-0.0482	0.0605	-	-	-	-1.0000	-	-	-0.0482	0.0605
T_{avg}	(3,1,2) (2,1,1) ₁₂	Seasonal	0.9692	-0.2214	0.0184	-	-	-1.6557	0.6560	-	-	-
		Nonseasonal	-0.0707	0.0927	-	-	-	-0.9723	-	-	-0.0707	0.0927
T_{max}	(3,1,2) (2,1,1) ₁₂	Seasonal	0.9377	-0.1725	0.0154	-	-	-1.6136	0.6203	-	-	-
		Nonseasonal	-0.0961	0.0244	-	-	-	-0.9992	-	-	-0.0961	0.0244
E_o	(2,1,5) (2,1,1) ₁₂	Seasonal	-0.1266	0.6175	-	-	-	-0.5577	-0.7155	0.4327	-0.1447	-0.0148
		Nonseasonal	0.1487	-0.1042	-	-	-	-0.9210	-	-	0.1487	-0.1042
S_o	(5,1,3) (2,1,3) ₁₂	Seasonal	-1.0384	-0.8514	0.0600	-0.0779	-0.0676	0.2856	-0.0353	-0.8846	-	-
		Nonseasonal	-0.576	-0.8670	-	-	-	-0.4308	0.5696	-0.9059	-0.576	-0.8670
H_o	(4,1,2) (5,1,2) ₁₂	Seasonal	-0.8294	0.0325	0.008	0.0839	-	-0.0415	-0.8815	-	-	-
		Nonseasonal	-1.0158	-0.3057	-0.1495	-0.1191	-0.1211	0.0613	-0.6850	-	-1.0158	-0.3057

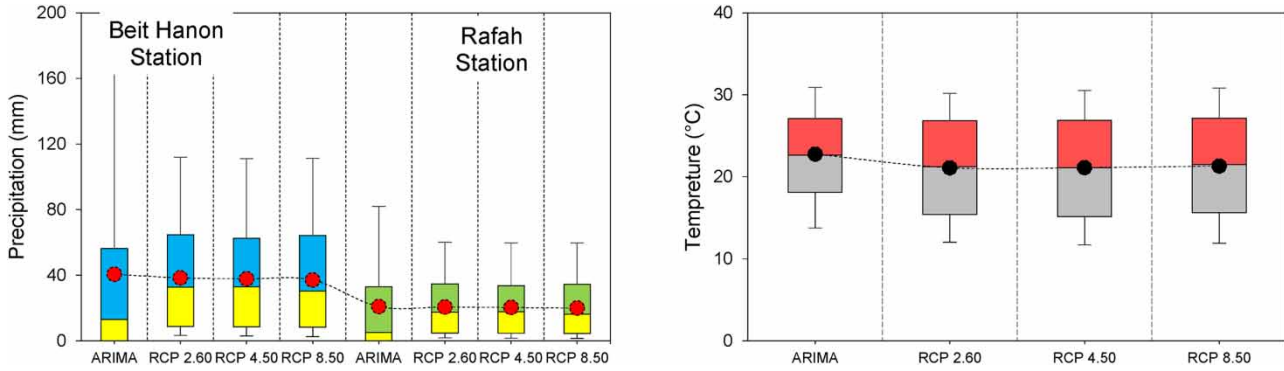


Figure 9 | Comparison between the ARIMA model output and RCPs of the ensemble GCM of CIMP5 outputs.

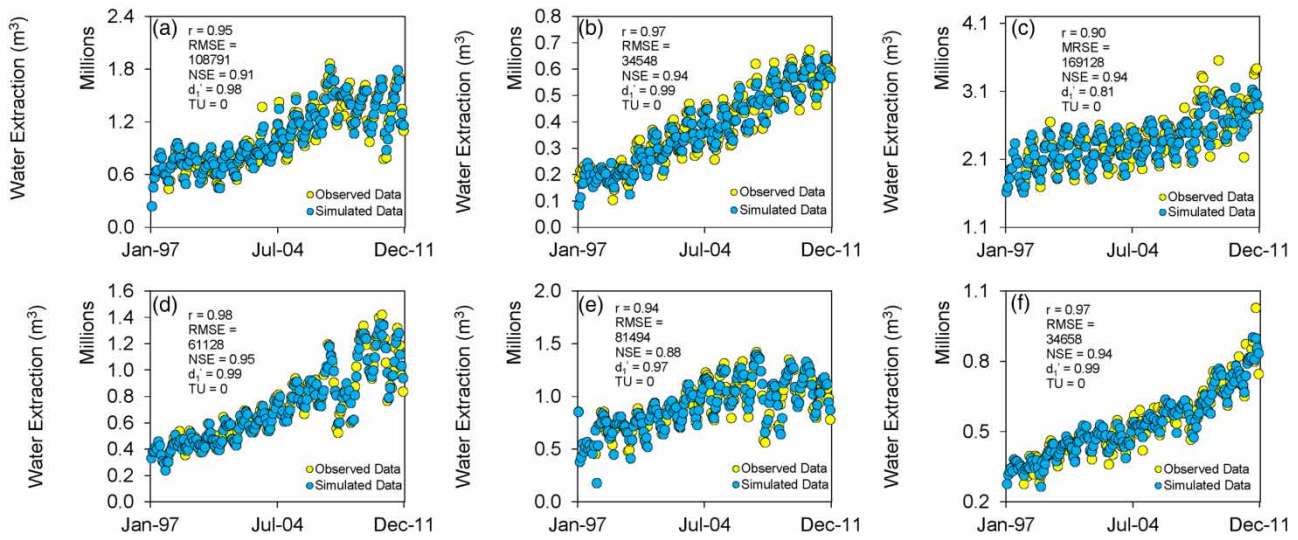


Figure 10 | Groundwater extraction for (a) Beit Hanon, (b) Beit Lahia, (c) Gaza, (d) Middle Gaza, (e) Khanyounis, and (f) Rafah.

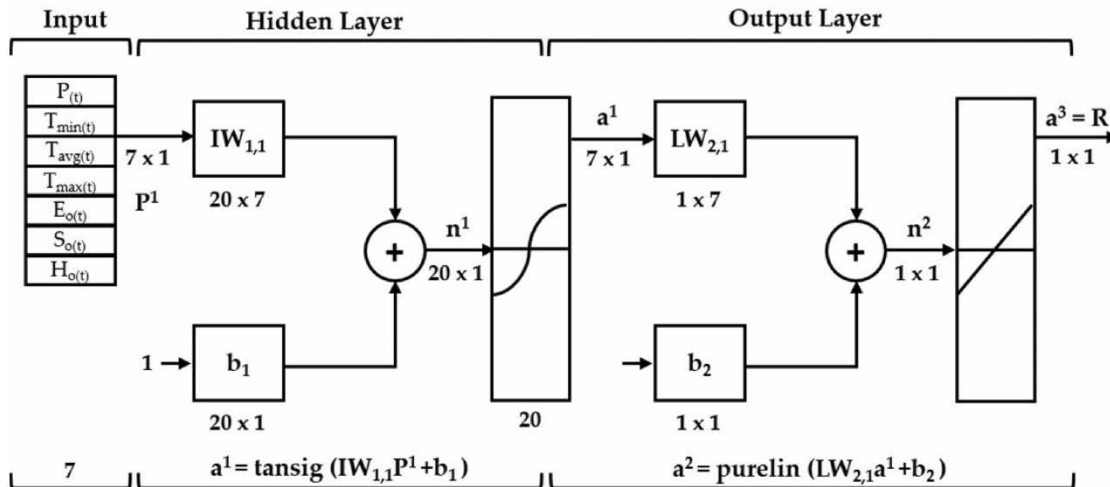


Figure 11 | Structure of the artificial MLP networks for the groundwater level of the Gaza coastal aquifer.

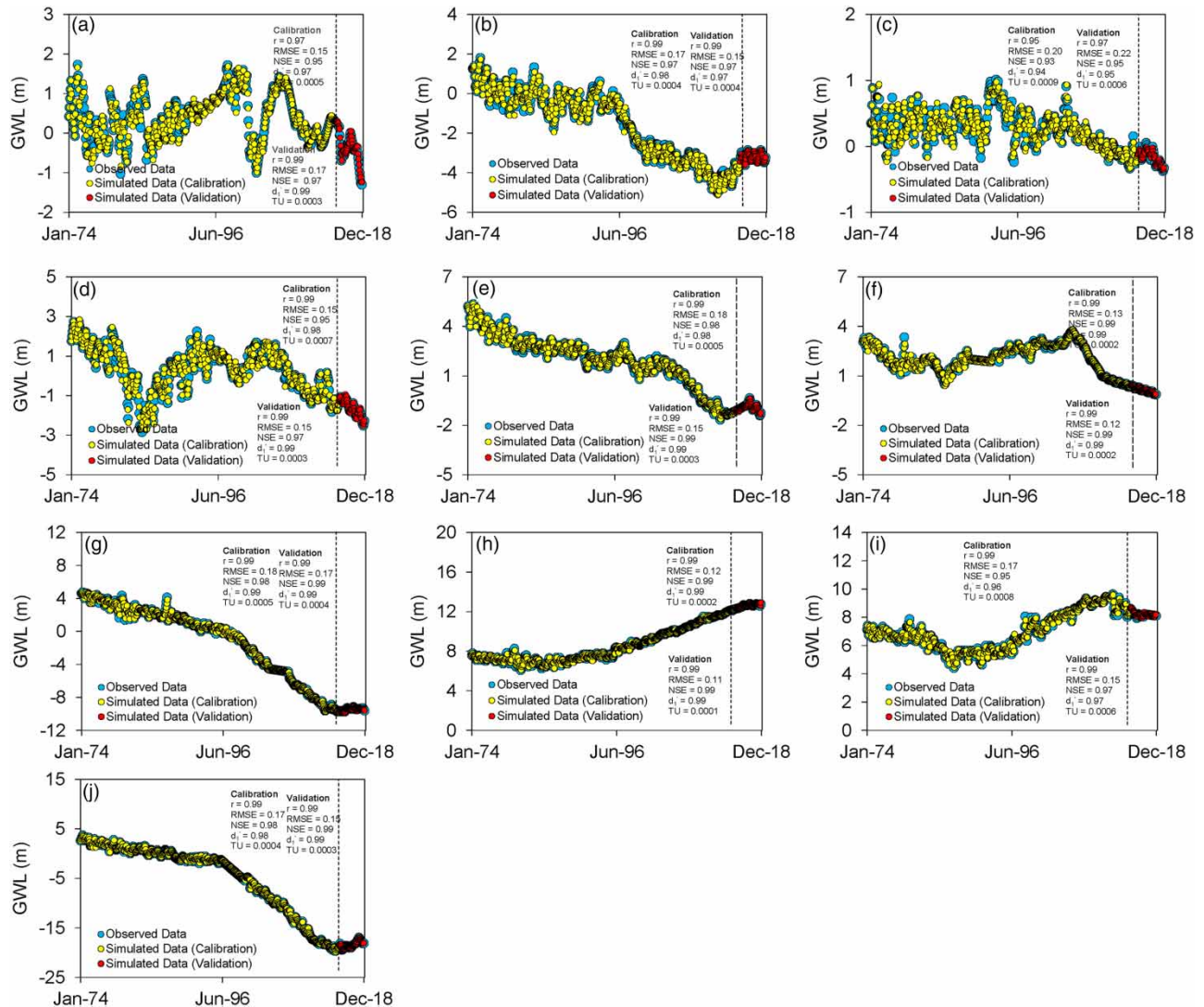


Figure 12 | Groundwater calibration and validation for (a) C/48, (b) E/45, (c) G/24B, (d) F/68B, (e) S/15, (f) L/86, (g) L/66, (h) N/12, (i) N/16, and (j) P/48A.

the chloride concentration to an acceptable level. The model predicts that obtained groundwater from the Gaza coastal aquifer will rise from 124 million cubic meters in 2020 to around 191 million cubic meters in 2040, with an annual increase rate of about 3%. The groundwater simulation findings, as shown in Figure 14, show that the groundwater-level drop is between -0.38 and -18.49 m below the MSL in 2020 and between -1.13 and -27.77 m below the MSL in 2040.

The simulation of the groundwater recovery as a result of the new water resource interventions is shown in Figure 15 for the southern region of the Gaza Strip, which exhibits critical deterioration in the coastal aquifer.

The simulation results show that using desalinated saltwater and treated wastewater instead of groundwater over-pumping operations results in a considerable 82–91% increase in the groundwater level.

6. CONCLUSION

The groundwater contained in the coastal aquifers is the prime resource for water supply in the Mediterranean region. The water supply of the Gaza Strip is in jeopardy due to the potential of extreme climate, as well as the increase in

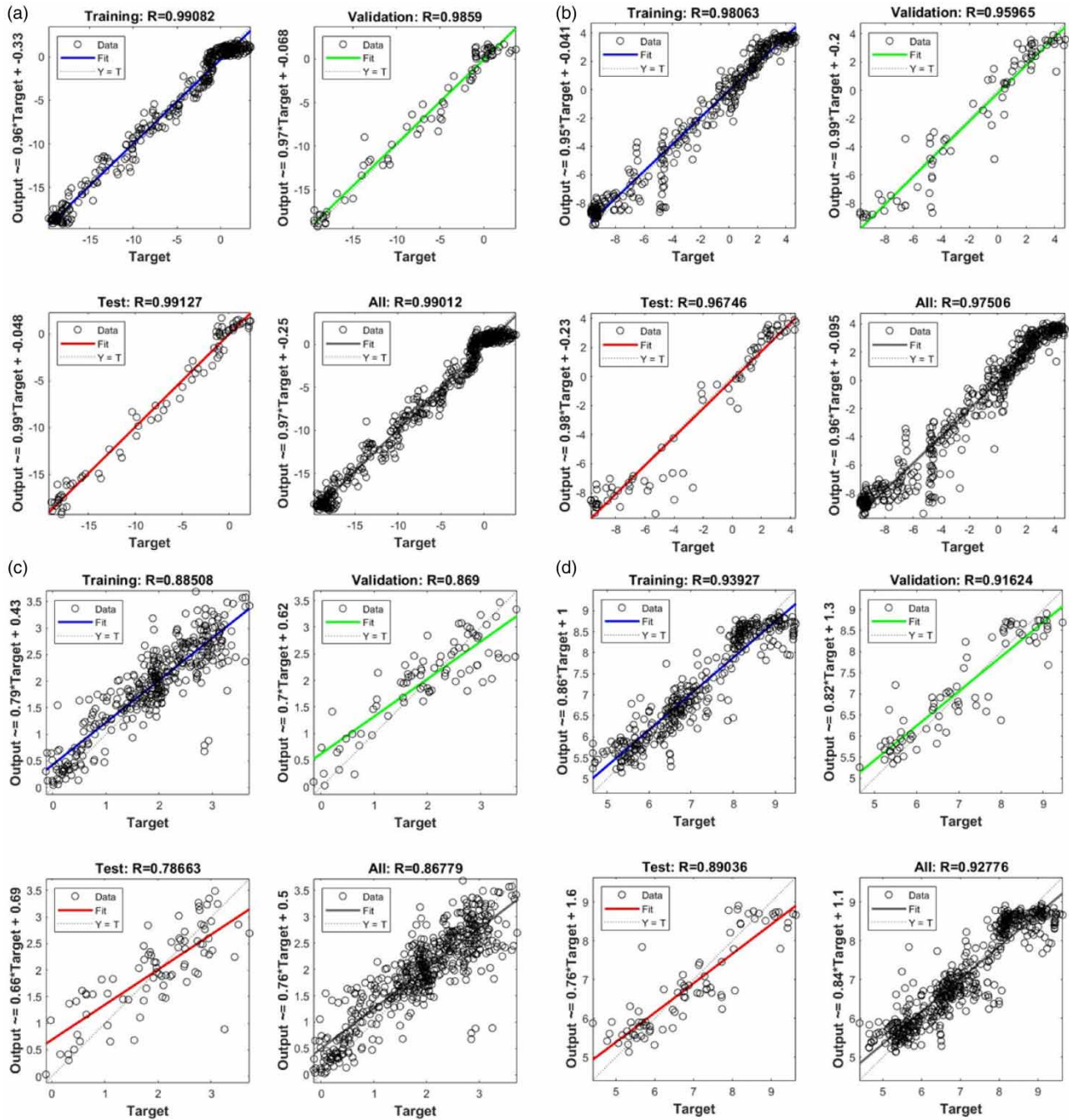


Figure 13 | Groundwater calibration and validation for (a) P/A48, (b) L/66, (c) L/86, and (d) N/16.

demand for water services as a result of exponential population growth. The future climate projection refers to an increase by +1 °C by the end of 2040 and by about +4 °C by the end of 2099 when compared to the historical temperature of 1975–2005. In addition, variation in the total monthly precipitation is expected to vary between –5% within 2006–2036 and –25% within 2068–2098. As a result, the Gaza coastal aquifer is projected to be under the critical conditions of overuse and imbalance where the simulation refers to a drop in the groundwater table reach to –28 m by the year 2040. The necessity for urgent intervention to sustain the groundwater resource in the Gaza Strip has directed

Table 2 | Performance testing parameters for the groundwater wells

Wells	Calibration					Validation				
	<i>r</i>	<i>RMSE</i>	<i>NSE</i>	<i>d</i> ₁	<i>TU</i>	<i>r</i>	<i>RMSE</i>	<i>NSE</i>	<i>d</i> ₁	<i>TU</i>
C/48	0.97	0.15	0.95	0.97	0.0005	0.99	0.17	0.97	0.99	0.0003
E/45	0.99	0.17	0.97	0.98	0.0004	0.99	0.15	0.97	0.97	0.0004
G/24B	0.95	0.20	0.93	0.94	0.0009	0.97	0.22	0.95	0.95	0.0006
F/68B	0.99	0.15	0.95	0.98	0.0007	0.99	0.15	0.97	0.99	0.0003
S/15	0.99	0.18	0.98	0.98	0.0005	0.99	0.15	0.99	0.99	0.0003
L/86	0.99	0.13	0.99	0.99	0.0002	0.99	0.12	0.99	0.99	0.0002
L/66	0.99	0.18	0.98	0.99	0.0005	0.99	0.17	0.99	0.99	0.0004
N/12	0.99	0.12	0.99	0.99	0.0002	0.99	0.11	0.99	0.99	0.0001
N/16	0.99	0.17	0.95	0.96	0.0008	0.99	0.15	0.97	0.97	0.0006
P/48A	0.99	0.17	0.98	0.98	0.0004	0.99	0.15	0.99	0.99	0.0003

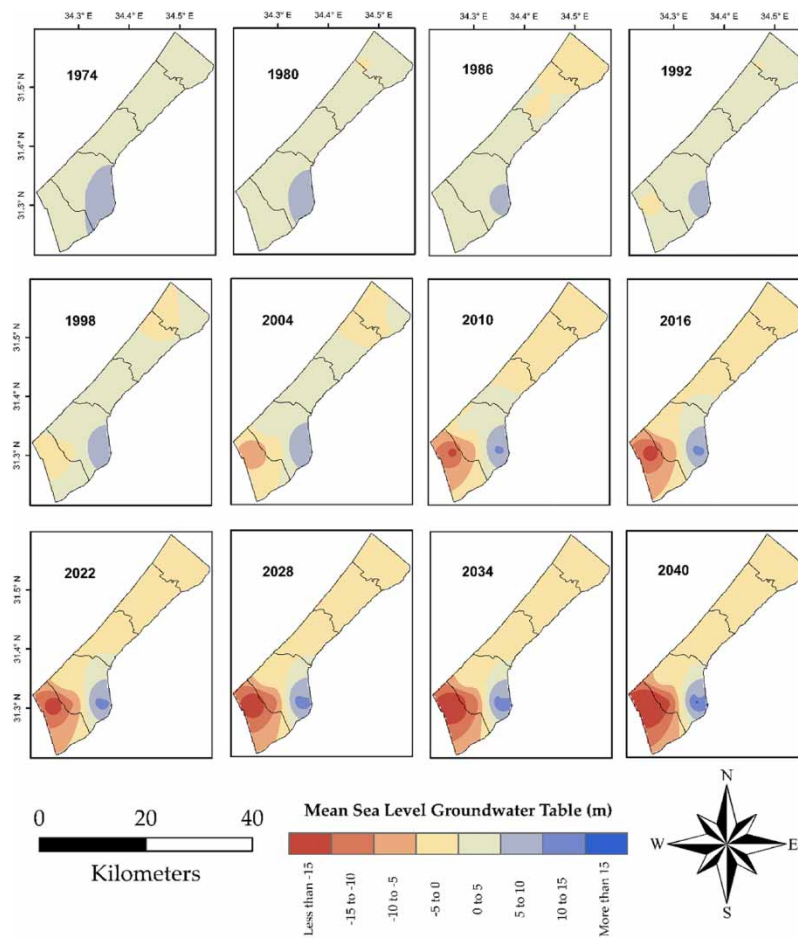


Figure 14 | Groundwater-level expectations for the Gaza coastal aquifer.

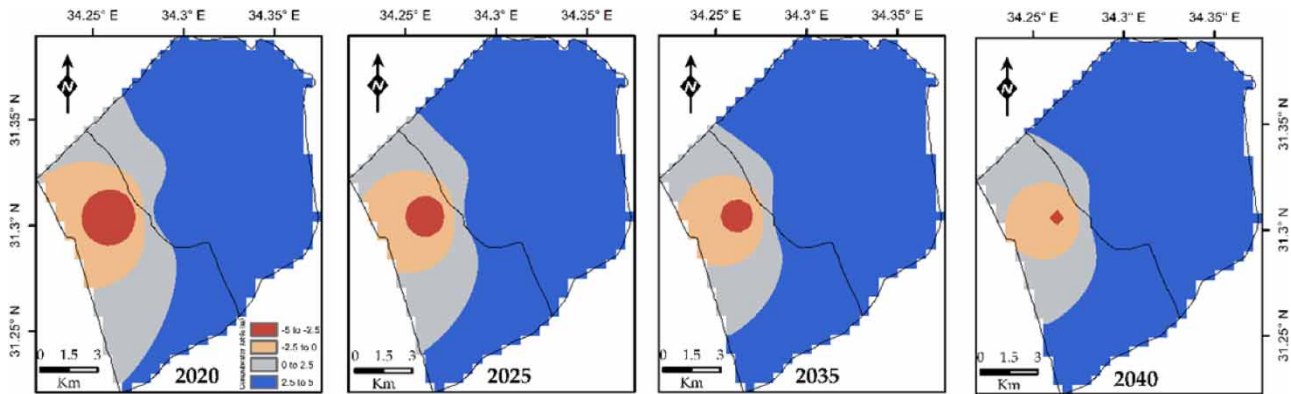


Figure 15 | Recovery scenarios of the groundwater of the Gaza coastal aquifer.

enterprises toward using the nontraditional water resources produced from seawater desalination and wastewater treatment, especially in the southern governorates of the Gaza Strip where the groundwater resource is overexploited. The simulation outputs for the process of compensation for the deficit in the water supply through the non-conventional water resources showed an optimized recovery in the groundwater level where the drop in the groundwater level is expected to be less than -5 m below the MSL.

CONFLICT OF INTEREST

The authors declare no conflict of interest.

DATA AVAILABILITY STATEMENT

All relevant data are included in the paper or its Supplementary Information.

REFERENCES

- Abualtayef, M., Al-Najjar, H., Mogheir, Y. & Seif, A. K. 2016 Numerical modeling of brine disposal from Gaza central seawater desalination plant. *Arabian Journal of Geosciences* **9** (10), 572.
- Abuatayef, M., Kahail, A., Al-Najjar, H. & AbuShbak, T. 2020 Applicability of using reverse osmosis membrane technology for wastewater reclamation in the Gaza strip. *The Journal of Engineering Research (TJER)* **17** (1), 11–23.
- Adamowski, J. & Chan, F. H. 2011 A wavelet neural network conjunction model for groundwater level forecasting. *Journal of Hydrology* **407** (1–4), 28–40.
- Adamowski, J., Chan, H. F., Prasher, S. O., Ozga-Zielinski, B. & Sliusarieva, A. 2012 Comparison of multiple linear and nonlinear regression, autoregressive integrated moving average, artificial neural network, and wavelet artificial neural network methods for urban water demand forecasting in Montreal, Canada. *Water Resources Research* **48**, 273–279.
- Afan, H. A., El-Shafie, A., Yaseen, Z. M., Hameed, M. M., Wan Mohtar, W. H. M. & Hussain, A. 2015 ANN-based sediment prediction model utilizing different input scenarios. *Water Resources Management* **29** (4), 1231–1245.
- Al-Najjar, H., Ceribasi, G., Dogan, E., Abualtayef, M., Qahman, K. & Shaqfa, A. 2020 Stochastic time-series models for drought assessment in the Gaza Strip (Palestine). *Journal of Water and Climate Change* **11** (S1), 85–114.
- Al-Najjar, H., Ceribasi, G. & Ceyhunlu, A. I. 2021a Effect of unconventional water resources interventions on the management of Gaza coastal aquifer in Palestine. *Journal of Water Supply* **21** (8), 4205–4218.
- Al-Najjar, H., Ceribasi, G., Dogan, E., Qahman, K., Abualtayef, M. & Ceyhunlu, A. I. 2021b Statistical modeling of spatial and temporal vulnerability of groundwater level in the Gaza Strip (Palestine). *H₂Open Journal* **4** (1), 352–365.
- Anderson, D. J. 2017 *Coastal Groundwater and Climate Change*. WRL Technical Report 2017/4. Water Research Laboratory, University of New South Wales, School of Civil Engineering.
- Barzegar, R., Fijani, E., Asghari Moghaddam, A. & Tziritis, E. 2017 Forecasting of groundwater level fluctuations using ensemble hybrid multi-wavelet neural network-based models. *Science of the Total Environment* **599–600**, 20–31.
- Bazrafshan, O., Salajegheh, A., Bazrafshan, J., Mahdavi, M. & Marj, A. F. 2015 Hydrological drought forecasting using ARIMA models (case study: Karkheh Basin). *Ecopersia* **3** (3), 1099–1117.
- Bishop, C. M. 1995 *Neural Networks for Pattern Recognition*. Oxford University Press, Inc., New York, NY, USA.
- Box, G. E. P. & Jenkins, G. M. 1970 *Time Series Analysis, Forecasting and Control*, rev. edn. Holden-Day, San Francisco, CA, USA.
- Box, G. E. P. & Jenkins, G. M. 1976 *Time Series Analysis: Forecasting and Control*, rev. edn. Holden-Day, San Francisco, CA, USA.

- Box, G. E. P., Jenkins, G. M. & Reinsel, G. C. 2008 *Time Series Analysis: Forecasting and Control*, 4th edn. Wiley Series in Probability and Statistics, Wiley, Hoboken, NJ, USA.
- Butler, J. J., Stotler, J. R. L., Whittemore, D. O. & Reboulet, E. C. 2013 Interpretation of water-level changes in the high plains aquifer in western Kansas. *Groundwater* **51** (2), 180–190.
- Chang, F. J., Chang, L. C., Huang, C. W. & Kao, I. F. 2016 Prediction of monthly regional groundwater levels through hybrid soft-computing techniques. *Journal of Hydrology* **541**, 965–976.
- Chatfield, C. 2008 *The Analysis of Time Series: An Introduction*, 6th edn. A CRC Press Company of Taylor and Francis Group, New York, NY, USA.
- Chen, L. H., Chen, C. T. & Lin, D. W. 2011 Application of integrated back-propagation network and self-organizing map for groundwater level forecasting. *Journal of Water Resources Planning and Management* **137** (4), 352–365.
- Djebbouai, S. & Souag-Gamane, D. 2016 Drought forecasting using neural networks, wavelet neural networks, and stochastic models: case of the Algerois Basin in North Algeria. *Water Resources Management* **30** (7), 2445–2464.
- Djurovic, N., Domazet, M., Stricevic, R., Pocuca, V., Spalevic, V., Pivic, R., Gregoric, E. & Domazet, U. 2015 Comparison of groundwater level models based on artificial neural networks and ANFIS. *The Scientific World Journal* **2015**, 1–13.
- Dogrul, E., Brush, C. & Kadir, T. 2016 Groundwater modeling in support of water resources management and planning under complex climate, regulatory, and economic stresses. *Water* **8** (12), 592.
- Ebrahimi, H. & Rajaei, T. 2017 Simulation of groundwater level variations using wavelet combined with neural network, linear regression and support vector machine. *Global and Planetary Change* **148**, 181–191.
- Emamgholizadeh, S., Moslemi, K. & Karami, G. 2014 Prediction the groundwater level of Bastam Plain (Iran) by artificial neural network (ANN) and adaptive neuro-fuzzy inference system (ANFIS). *Water Resources Management* **15**, 5433–5446.
- Ghose, D., Das, U. & Roy, P. 2018 Modeling response of runoff and evapotranspiration for predicting water table depth in arid region using dynamic recurrent neural network. *Groundwater for Sustainable Development* **6**, 263–269.
- Gladden, I. A. & Park, N. S. 2016 *Coastal Groundwater Development: Challenges and Opportunities*, 1st edn. CRC Press, Boca Raton, FL, USA.
- Gong, Y., Zhang, Y., Lan, S. & Wang, H. 2016 A comparative study of artificial neural networks, support vector machines and adaptive neuro fuzzy inference system for forecasting groundwater levels near Lake Okeechobee, Florida. *Water Resources Management* **30**, 375–391.
- Gopalakrishnan, T., Hasan, M. K., Haque, A. S., Jayasinghe, S. L. & Kumar, L. 2019 Sustainability of coastal agriculture under climate change. *Sustainability* **11** (24), 7200.
- Guzman, S. M., Paz, J. O., Tagert, M. L. M. & Mercer, A. E. 2019 Evaluation of seasonally classified inputs for the prediction of daily groundwater levels: NARX networks vs support vector machines. *Environmental Modelling and Assessment* **24**, 223–234.
- Haykin, S. 2009 *Neural Networks and Learning Machines*, 3rd edn. Pearson Education, Inc., Upper Saddle River, NJ, USA.
- He, Z., Zhang, Y., Guo, Q. & Zhao, X. 2014 Comparative study of artificial neural networks and wavelet artificial neural networks for groundwater depth data forecasting with various curve fractal dimensions. *Water Resources Management* **28**, 5297–5317.
- Hussain, M. I., Muscolo, A., Farooq, M. & Ahmad, W. 2019 Sustainable use and management of non-conventional water resources for rehabilitation of marginal lands in arid and semiarid environments. *Agricultural Water Management* **221**, 462–476.
- Jalalkamali, A., Sedghi, H. & Manshour, M. 2011 Monthly groundwater level prediction using ANN and neuro-fuzzy models: a case study on Kerman plain, Iran. *Journal of Hydroinformatics* **13** (4), 867–876.
- Juan, C., Genxu, W. & Tianxu, M. 2015 Simulation and prediction of suprapermafrost groundwater level variation in response to climate change using a neural network model. *Journal of Hydrology* **529**, 1211–1220.
- Karimi, L., Motagh, M. & Entezam, I. 2019 Modeling groundwater level fluctuations in Tehran aquifer: results from a 3D unconfined aquifer model. *Groundwater for Sustainable Development* **8**, 439–449.
- Kashyap, R. L. & Rao, A. R. 1976 Dynamic stochastic models from empirical data. In: *Mathematics in Science and Engineering*, Vol. 122 (Kashyap, A., ed.). Academic Press, Inc., London, UK, p. 334.
- Khaki, M., Yusoff, I. & Islami, N. 2015 Simulation of groundwater level through artificial intelligence system. *Environmental Earth Sciences* **73** (12), 8357–8367.
- Khalil, B., Broda, S., Adamowski, J., Ozga-Zielinski, B. & Donohoe, A. 2015 Short-term forecasting of groundwater levels under conditions of mine-tailings recharge using wavelet ensemble neural network models. *Journal of Hydrogeology*. **23**, 121–141.
- Khorasani, M., Ehteshami, M., Ghadimi, H. & Salari, M. 2016 Simulation and analysis of temporal changes of groundwater depth using time series modeling. *Modeling Earth Systems and Environment* **2** (2), 1–10.
- Koopmans, L. H. 1974 *The Spectral Analysis of Time Series*. Academic Press, Inc., New York, NY, USA.
- Kottogoda, N. T. 1990 *Stochastic Water Resources Technology*, 1st edn. Palgrave Macmillan, London, UK, p. 384.
- Kouziokas, G. N., Chatzigeorgiou, A. & Perakis, K. 2018 Multilayer feed forward models in groundwater level forecasting using meteorological data in public management. *Water Resources Management* **32**, 5041–5052.
- Kumbuyo, C. P., Yasuda, H., Kitamura, Y. & Shimizu, K. 2014 Fluctuation of rainfall time series in Malawi: an analysis of selected areas. *Geofizika* **31**, 15–12.
- Lee, S., Lee, K. K. & Yoon, H. 2019 Using artificial neural network models for groundwater level forecasting and assessment of the relative impacts of influencing factors. *Journal of Hydrogeology* **27**, 567–579.

- Maier, H. R., Jain, A., Dandy, G. C. & Sudheer, K. P. 2010 Methods used for the development of neural networks for the prediction of water resource variables in river systems: current status and future directions. *Environmental Modelling Software* **25**, 891–909.
- Mirzavand, M. & Ghazavi, R. 2015 A stochastic modelling technique for groundwater level forecasting in an arid environment using time series methods. *Water Resources Management* **29** (4), 1315–1328.
- Mogaji, K. A., Lim, H. S. & Abdullah, K. 2015 Regional prediction of groundwater potential mapping in a multifaceted geology terrain using GIS-based Dempster–Shafer model. *Arabian Journal of Geosciences* **8**, 3235–3258.
- Mohanty, S., Jha, M. K., Kumar, A. & Sudheer, K. P. 2010 Artificial neural network modeling for groundwater level forecasting in a river island of Eastern India. *Water Resources Management* **24**, 1845–1865.
- Mohanty, S., Jha, M. K., Raul, S. K., Panda, R. K. & Sudheer, K. P. 2015 Using artificial neural network approach for simultaneous forecasting of weekly groundwater levels at multiple sites. *Water Resources Management* **29** (15), 5521–5532.
- Moosavi, V., Vafakhah, M., Shirmohammadi, B. & Ranjbar, M. 2013 Optimization of wavelet-ANFIS and wavelet-ANN hybrid models by Taguchi method for groundwater level forecasting. *Arabian Journal for Science and Engineering* **39** (3), 1785–1796.
- Myronidis, D., Ioannou, K., Fotakis, D. & Dörflinger, G. 2018 Streamflow and hydrological drought trend analysis and forecasting in Cyprus. *Water Resources Management* **32** (5), 1759–1776.
- Nourani, V. & Mousavi, S. 2016 Spatiotemporal groundwater level modeling using hybrid artificial intelligence-meshless method. *Journal of Hydrology* **536**, 10–25.
- Nourani, V., Ejlali, R. G. & Alami, M. T. 2011 Spatiotemporal groundwater level forecasting in coastal aquifers by hybrid artificial neural network-geostatistics model: a case study. *Environmental Engineering Science* **28** (3), 217–228.
- Nourani, V., Alami, M. T. & Daneshvar Vousoughi, F. 2015 Wavelet-entropy data pre-processing approach for ANN-based groundwater level modeling. *Journal of Hydrology* **524**, 255–269.
- Otkin, J. A., Svoboda, M., Hunt, E. D., Ford, T. W., Anderson, M. C., Hain, C. & Basara, J. B. 2018 Flash droughts: a review and assessment of the challenges imposed by rapid-onset droughts in the United States. *Bulletin of the American Meteorological Society* **99**, 911–919.
- Patle, G. T., Singh, D. K., Sarangi, A., Rai, A., Khanna, M. & Sahoo, R. N. 2015 Time series analysis of groundwater levels and projection of future trend. *Journal of the Geological Society of India* **85**, 232–242.
- PCBS. 2020 *Estimated Population in the Palestinian Territory Mid-Year by Governorate, 1997–2021*. IOP Publishing Physics Web. Available from: <http://www.pcbs.gov.ps> (accessed 25 December 2020).
- Polyak, I. 1996 *Computational Statistics in Climatology*. Oxford University Press, Oxford.
- PWA 2011 *The Comparative Study of Options for an Additional Supply of Water for the Gaza Strip (CSO-G), The Updated Final Report*. Palestinian Water Authority.
- PWA 2012 Palestinian water sector: status summary report. In *Preparation for the Meeting of the Ad Hoc Liaison Committee (AHLIC)*, 23 September 2012. Palestinian Water Authority, New York.
- PWA 2013 *National Water and Wastewater Policy and Strategy for Palestine: Toward Building a Palestinian State from Water Perspective*. Palestinian Water Authority.
- PWA 2014 *Gaza Strip: No Clean Drinking Water, No Enough Energy, and Threatened Future*. Palestinian Water Authority.
- PWA 2015 *Gaza Strip: Desalination Facility Project: Necessity, Politics and Energy*. Palestinian Water Authority.
- Rakhshandehroo, G. R., Vaghefi, M. & Asadi Aghbolaghi, M. 2012 Forecasting groundwater level in Shiraz plain using artificial neural networks. *Arabian Journal for Science and Engineering* **37**, 1871–1883.
- Representative Concentration Pathways (RCPs) 2019 IPCC. Retrieved 13 February.
- Sahoo, S. & Jha, M. K. 2013 Groundwater-level prediction using multiple linear regression and artificial neural network techniques, a comparative assessment. *Journal of Hydrogeology* **21**, 1865–1887.
- Sakizadeh, M., Mohamed, M. M. A. & Klammmler, H. 2019 Trend analysis and spatial prediction of groundwater levels using time series forecasting and a novel spatio-temporal method. *Water Resources Management* **33**, 1425–1437.
- Schiermeier, Q. 2018 Droughts, heatwaves and floods: how to tell when climate change is to blame. *Nature* **560**, 20–22.
- Shahin, M., Van Oorschot, H. J. L. & De Lange, S. J. 1993 *Statistical Analysis in Water Resources Engineering*. A.A. Balkema, Rotterdam, The Netherlands, p. 394.
- Sharma, P., Machiwal, D. & Jha, M. K. 2019 Overview, current status, and future prospect of stochastic time series modeling in subsurface hydrology. *GIS and Geostatistical Techniques for Groundwater Science*. Elsevier, The Netherlands, pp. 133–151.
- Shirmohammadi, B., Vafakhah, M., Moosavi, V. & Moghaddamnia, A. 2013 Application of several data-driven techniques for predicting groundwater level. *Water Resources Management* **27** (2), 419–432.
- Singh, A. 2014 Simulation and optimization modeling for the management of groundwater resources. II: combined applications. *Journal of Irrigation and Drainage Engineering* **140** (4), 1–9.
- Sun, Y., Wendi, D., Kim, D. E. & Liang, S. 2016 Technical note: application of artificial neural networks in groundwater table forecasting – a case study in a Singapore swamp forest. *Hydrology and Earth System Sciences* **20** (4), 1405–1412.
- Takafuji, E. H. D. M., Rocha, M. M. D. & Manzione, R. L. 2018 Groundwater level prediction/forecasting and assessment of uncertainty using SGS and ARIMA models: a case study in the Bauru Aquifer System (Brazil). *Natural Resources Research* **28**, 487–503.
- Tang, Y., Zang, C., Wei, Y. & Jiang, M. 2019 Data-driven modeling of groundwater level with least-square support vector machine and spatial-temporal analysis. *Geotechnical Geological Engineering* **37**, 1661–1670.

- Taormina, R., Chau, K. & Sethi, R. 2012 Artificial neural network simulation of hourly groundwater levels in a coastal aquifer system of the Venice lagoon. *Engineering Applications of Artificial Intelligence* **25** (8), 1670–1676.
- Tapoglou, E., Karatzas, G. P., Trichakis, I. C. & Varouchakis, E. A. 2014 A spatio-temporal hybrid neural network-Kriging model for groundwater level simulation. *Journal of Hydrology* **519**, 3193–3203.
- Thangarajan, M. & Singh, V. P. 2016 *Groundwater Assessment, Modeling, and Management*, 1st edn. CRC Press, Boca Raton.
- Tong, H. 1990 *Nonlinear Time Series: A Dynamical System Approach*. Oxford University Press, Oxford.
- Trichakis, I. C., Nikolos, I. K. & Karatzas, G. P. 2011 Artificial neural network (ANN) based modeling for Karstic groundwater level simulation. *Water Resources Management* **25**, 1143–1152.
- UfM 2011 *Gaza Desalination Project: The Largest Single Facility to be Built in Gaza*. Union for the Mediterranean Secretariat.
- UN 2012 *Gaza 2020: A Livable Place? A Report by the United Nations Country Team in the Occupied Palestinian Territory, The United Nations*.
- Wen, X., Feng, Q., Deo, R. C., Wu, M. & Si, J. 2017 Wavelet analysis–artificial neural network conjunction models for multi-scale monthly groundwater level predicting in an arid inland river basin, northwestern China. *Hydrology Research* **48** (6), 1710–1729.
- Yan, Q. & Ma, C. 2016 Application of integrated ARIMA and RBF network for groundwater level forecasting. *Environmental Earth Sciences* **75** (5), 396.
- Yang, Q., Hou, Z., Wang, Y., Zhao, Y. & Delgado, J. 2015 A comparative study of shallow groundwater level simulation with WA-ANN and ITS model in a coastal island of south China. *Arabian Journal of Geosciences* **8** (9), 6583–6593.
- Ye, G., Chou, L. M., Yang, S., Wu, J., Liu, P. & Jin, C. 2015 Is integrated coastal management an effective framework for promoting coastal sustainability in China's coastal cities? *Marine Policy* **56**, 48–55.
- Yeh, H. D. & Chang, Y. C. 2013 Recent advances in modeling of well hydraulics. *Advances in Water Resources* **51**, 27–51.
- Ying, Z., Wenxi, L., Haibo, C. & Jiannan, L. 2014 Comparison of three forecasting models for groundwater levels: a case study in the semiarid area of west Jilin Province, China. *Journal of Water Supply: Research and Technology-Aqua* **8**, 671–683.
- Yoon, H., Jun, S. C., Hyun, Y., Bae, G. O. & Lee, K. K. 2011 A comparative study of artificial neural networks and support vector machines for predicting groundwater levels in a coastal aquifer. *Journal of Hydrology* **396** (1), 128–138.
- Yoon, H., Hyun, Y., Ha, K., Lee, K. K. & Kim, G. B. 2016 A method to improve the stability and accuracy of ANN- and SVM-based time series models for long-term groundwater level predictions. *Computers and Geosciences* **90**, 144–155.
- Yu, H., Wen, X., Feng, Q., Deo, R. C., Si, J. & Wu, M. 2018 Comparative study of hybrid-wavelet artificial intelligence models for monthly groundwater depth forecasting in extreme arid regions, northwest China. *Water Resources Management* **32** (1), 301–323.
- Zekri, S., Madani, K., Bazargan-Lari, M. R., Kotagama, H. & Kalbus, E. 2017 Feasibility of adopting smart water meters in aquifer management: an integrated hydro-economic analysis. *Agricultural Water Management* **181**, 85–93.
- Zhou, T., Wang, F. & Yang, Z. 2017 Comparative analysis of ANN and SVM models combined with wavelet preprocess for groundwater depth prediction. *Water* **9** (10), 781.

First received 17 August 2021; accepted in revised form 24 March 2022. Available online 8 April 2022